

Deep Learning for Over-the-Air Non-Orthogonal Signal Classification

Tongyang Xu and Izzat Darwazeh

Department of Electronic and Electrical Engineering, University College London, London, UK

Email: tongyang.xu.11@ucl.ac.uk, i.darwazeh@ucl.ac.uk

Abstract—Non-cooperative communications, where a receiver can automatically distinguish and classify transmitted signal formats prior to detection, are desirable for low-cost and low-latency systems. This work focuses on the deep learning enabled blind classification of multi-carrier signals covering their orthogonal and non-orthogonal varieties. We define Type-I signals with large feature diversity and Type-II signals with strong feature similarity. We evaluate time-domain and frequency-domain convolutional neural network (CNN) models with wireless channel/hardware impairments. Experimental systems are designed and tested, using software defined radio (SDR) devices, operated for different signal formats in line-of-sight and non-line-of-sight communication link scenarios. Testing, using four different time-domain CNN models, showed the pre-trained CNN models to have limited efficiency and utility due to the mismatch between the analytical/simulation and practical/real-world environments. Transfer learning, which is an approach to fine-tune learnt signal features, is applied based on measured over-the-air time-domain signal samples. Experimental results indicate that transfer learning based CNN can efficiently distinguish different signal formats for Type-I in both line-of-sight and non-line-of-sight scenarios relative to the non-transfer-learning approaches. Type-II signals are not identified correctly in the experiment even with the transfer learning assistance leading to potential applications in secure communications.

Index Terms—Non-cooperative, signal classification, deep learning, conventional neural network (CNN), transfer learning, non-orthogonal, SEFDM, waveform, software defined radio, secure communication.

I. INTRODUCTION

In legacy systems, to facilitate successful communications, both transmitter and receiver should cooperatively work on the basis of mutually-known protocols. This is at the cost of extra control overhead, time delay and inaccuracy due to the time-variant wireless channels. Therefore, non-cooperative communications are preferred in low-power low-latency communication scenarios, where a receiver can automatically distinguish signal formats.

Recent pioneering work in [1] considered the use of deep learning to extract signal features and practically revealed the possibility of using convolutional neural network (CNN) for single-carrier modulation classification. This motivated other research teams to investigate similar techniques for multi-carrier signals such as orthogonal frequency division multiplexing (OFDM) [2], [3]. Due to the orthogonal sub-carrier packing feature, OFDM signals avoid internal signal interference leading to robust and accurate classification. However, for non-orthogonal signals such as frequency-domain spec-

trally efficient frequency division multiplexing (SEFDM) [4] and time-domain faster than Nyquist (FTN) [5], sub-carriers or time samples are packed closer and non-orthogonally resulting in self-created interference. This intrinsic signal interference causes ambiguity and would significantly affect signal classification accuracy. This work will focus on the spectrally efficient SEFDM, since its flexible sub-carrier packing strategy [6] makes it well suited for non-cooperative communications.

Conventional CNN models are trained in this work using emulation data and later are tested on over-the-air data in practical software defined radio (SDR) devices. The trained CNN models work well in simulation but this might not be true for practical applications, since the training data and the real world data would have different environment features. Transfer learning [7] is an approach to speed up training via fine-tuning pre-trained models. Instead of making tremendous efforts on training a single neural network to deal with multi-task problems, transfer learning extracts learnt knowledge from a source task and then applies it to a target task with fast fine-tuning according to the target task environment. This strategy is fit for precision signal classification in condition-variant over-the-air signal communications.

This work will firstly study the features of non-orthogonal multi-carrier SEFDM signals. Then eight CNN models are trained off-line with the extensive considerations of analytical channel/hardware impairments. Moreover, an environment dependent transfer learning strategy is applied to the pre-trained CNN models. Finally, over-the-air signal transmissions in both line-of-sight (LOS) and non-line-of-sight (NLOS) scenarios are conducted with signal classifications using the trained CNN models and the transfer learning strategy.

The main contributions of this work are as the following.

- First time study on non-orthogonal multi-carrier signals classification using deep learning.
- Extensive investigations on non-orthogonal signal diversity and similarity.
- Over-the-air non-orthogonal signals classification.

II. FEATURES IN NON-ORTHOGONAL SIGNALS

The SEFDM signal saves spectral resources [6] when compared with OFDM due to its non-orthogonal sub-carrier packing. The basic mathematical format of SEFDM signals is

$$X_k = \frac{1}{\sqrt{N}} \sum_{n=1}^N s_n \exp\left(\frac{j2\pi nk\alpha}{N}\right), \quad (1)$$

where $\alpha = \Delta f \cdot T$ is the bandwidth compression factor, which determines the sub-carrier packing characteristics. The system is OFDM when $\alpha = 1$ while $\alpha < 1$ indicates SEFDM signals. Parameters N, n, k are the number of sub-carriers, sub-carrier index and time sample index, respectively.

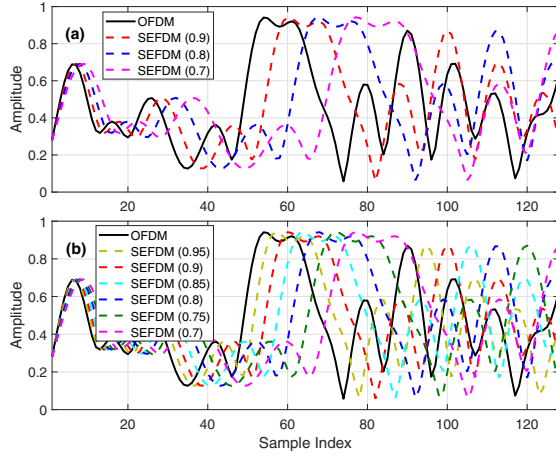


Fig. 1. Signal feature diversity and similarity visualization by modulating the same QPSK data. (a) Type-I signals. (b) Type-II signals.

The time samples for OFDM and SEFDM of variable bandwidth compression factors are illustrated in Fig. 1 where two types of signals are defined in the following. The number in the bracket of each item indicates bandwidth compression factors.

- **Type – I:** OFDM-QPSK, SEFDM-QPSK(0.9), SEFDM-QPSK(0.8), SEFDM-QPSK(0.7)
- **Type – II:** OFDM-QPSK, SEFDM-QPSK(0.95), SEFDM-QPSK(0.9), SEFDM-QPSK(0.85), SEFDM-QPSK(0.8), SEFDM-QPSK(0.75), SEFDM-QPSK(0.7)

Fig. 1(a) shows clearly the feature diversity among different SEFDM signals but with increasing similarity when signals have closer bandwidth compression factors in Fig. 1(b). Thus, classification of the Type-II signals is more challenging.

III. NEURAL NETWORK MODELLING

This work focuses on indoor communication scenarios, which have simple and relatively stable channel conditions after communication devices deployment, but with different channels for devices at different locations. In addition, indoor people movement would cause minor Doppler spread effect. All the impairments will be considered in the neural network (NN) modelling.

A. Dataset Generation

Work in [8] provides RadioML dataset, which aims at single-carrier modulation classifications. However, for multi-carrier SEFDM and OFDM signals, new datasets have to be generated. In this work, to make neural network modelling convincing, we generate random SEFDM/OFDM samples for both training dataset and testing dataset according to the parameters in Table I. Since multi-carrier IoT signals prefer

low order modulation formats for simplicity reasons, this work therefore focuses on QPSK modulation symbols.

Table I: Signal specifications

Parameter	Signal
Sampling frequency (kHz)	200
IFFT sample length	2048
Oversampling factor	8
No. of data sub-carriers	256
Bandwidth compression factor α	1,0.95,0.9,0.85,0.8,0.75,0.7
Modulation scheme	QPSK

Table II: Channel/hardware specifications

Parameter	Channel/Hardware
RF center frequency (MHz)	900
Simulation Es/N0 range (dB)	-20 ~ +50
Path delay (s)	[0 9e-6 1.7e-5]
Path relative power (dB)	[0 -2 -10]
Maximum Doppler frequency (Hz)	4
K-factor	4
Frequency offset (PPM)	2
Omni-directional antenna gain (dBi)	2

We emulate the analytical channel/hardware model in Table II partially following the work of [1], [8], in which an indoor wireless channel power delay profile (PDP) is defined. However, in our experiment, considering realistic indoor office environment, a time-variant wireless channel is configured with a greater maximum Doppler frequency of 4 Hz. In terms of hardware, this work uses the low-cost Analog Devices SDR PLUTO [9], which is supported by Matlab. Therefore, hardware related impairments have to be reconfigured based on the PLUTO devices. According to [10], a calibrated oscillator has a frequency offset of 2 parts per million (PPM), which will be emulated in the off-line neural network training.

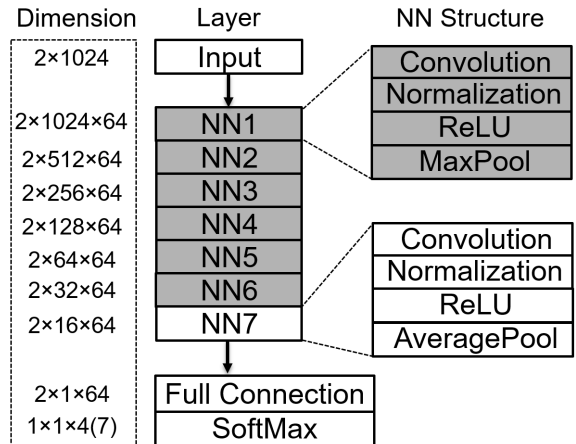


Fig. 2. CNN classifier neural network layer architecture.

B. Convolutional Neural Network

For the purpose of results reproducibility, the trained CNN layer architecture is presented in Fig. 2, in which seven NN

layers are stacked for feature extractions. Each of the first six NN layers is made up of four sub-layers, which are presented in the grey NN structure module. In the last NN layer, the MaxPool layer is replaced by the AveragePool layer. The classification is realized by a full connection layer and a SoftMax layer with cross-entropy loss function update. The dimension of each layer is presented in the left-side column. To avoid overfitting in the neural network training, a 50% dropout ratio is set. The maximum number of epochs is limited to 30 and the mini-batch size is 128. To learn comprehensively from the dataset, a learning rate of 0.01 is configured.

Table III: Training/validation datasets for time-domain CNN models.

Model	Training/validation datasets
time-CNN-1	Type-I
time-CNN-2	Type-I, channel/hardware model, $E_s/N_0=20$ dB
time-CNN-3	Type-II
time-CNN-4	Type-II, channel/hardware model, $E_s/N_0=20$ dB

Table IV: Training/validation datasets for frequency-domain CNN models.

Model	Training/validation datasets
fre-CNN-1	Fourier transform (time-CNN-1 datasets)
fre-CNN-2	Fourier transform (time-CNN-2 datasets)
fre-CNN-3	Fourier transform (time-CNN-3 datasets)
fre-CNN-4	Fourier transform (time-CNN-4 datasets)

We designed four time-domain training/validation datasets for Type-I and Type-II signals as presented in Table III. The datasets for time-CNN-1 and time-CNN-3 only consider signal intrinsic features while the other two datasets for time-CNN-2 and time-CNN-4 consider signal features, analytical channel/hardware impairments and additive white Gaussian noise (AWGN). In addition, we investigate the frequency-domain responses using fast Fourier transform (FFT) with the datasets presented in Table IV.

To separate SEFDM/OFDM symbols from time samples and QPSK symbols, a concept of frame is used here. In this case, one frame indicates one SEFDM/OFDM symbol. Each frame has 2048 time samples with the oversampling factor of eight. The receiver would receive frames with a random time delay relative to ideal frame reception and would randomly truncate 1024 consecutive time samples out of the 2048 samples. The training/testing would operate on the truncated 1024 samples and thus without synchronization requirement. The block diagrams of the employed training and testing strategies are illustrated in Fig. 3. It is noted that the E_s/N_0 information will not be used to train the CNN models.

Training is operated on an Intel(R) Xeon(R) Silver 4114 CPU (2 processors). In this work, following the information provided by Table III and Table IV, we generate 2200 frames for each signal class, in which 2000 frames are reserved for training and 200 frames are for validation. Thus, the

Table V: Testing datasets for time- frequency-domain CNN models.

Model	Testing datasets
time-CNN-1,2	Type-I, channel/hardware model, $E_s/N_0= -20:50$ dB
fre-CNN-1,2	Fourier transform (time-CNN-1,2 datasets)
time-CNN-3,4	Type-II, channel/hardware model, $E_s/N_0= -20:50$ dB
fre-CNN-3,4	Fourier transform (time-CNN-3,4 datasets)

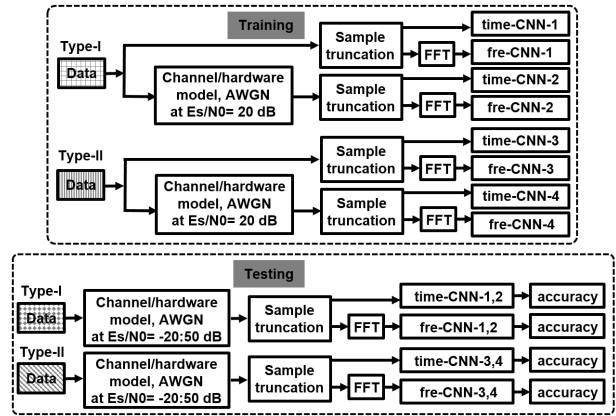


Fig. 3. Methodology of training and testing.

percentages of data for training and validation are around 91% and 9%, respectively. In addition, a separate dataset following the information provided by Table V, consisting of 800 frames for each signal class, is used for the neural network testing. For example, for Type-I signals, there are 8000 frames for training, 800 frames for validation and 3200 frames for testing. For Type-II signals, there are 14000 frames for training, 1400 frames for validation and 5600 frames for testing.

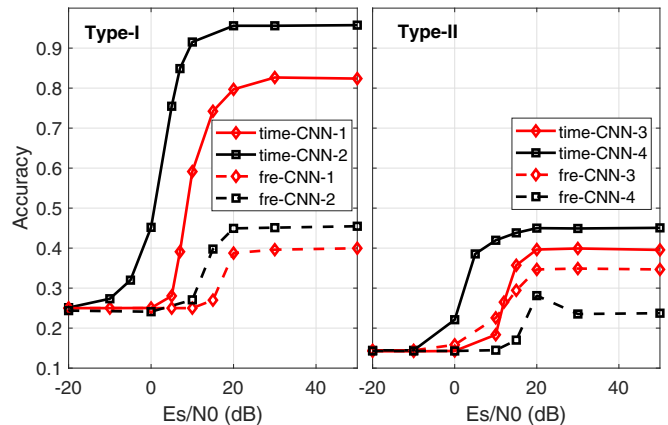


Fig. 4. Simulation signal classification accuracy for SEFDM signals.

In Fig. 4, it is clearly seen in Type-I signals that the time-CNN-2 model, which is trained based on signals and the analytical channel/hardware model, achieves the highest

accuracy. Unlike the time-CNN-2 model, time-CNN-1 is modelled using clean signals where carrier frequency offset, phase offset, time delay spread, Doppler spread, AWGN and any other channel/hardware related impairments are ignored at the training stage. This model would be vulnerable for testing in time-variant wireless channel environments resulting in reduced accuracy. However, for the frequency-domain CNN-1 and CNN-2 models show significantly decreased accuracy. It is inferred that for non-orthogonal signals, training on original time samples in deep learning CNN would gain higher accuracy than that of its frequency-domain responses. For Type-II signals in Fig. 4, due to higher signal feature similarity, the accuracy levels for both time-domain and frequency-domain CNN-3 and CNN-4 are worse than those in Type-I signals. It indicates that the signal feature similarity dominates the classification accuracy in Type-II signals rather than channel/hardware condition mismatches. But the time-domain CNN models still outperform their frequency-domain counterparts. Therefore, in the following experiment, only the time-domain neural network training methodology is applied.

IV. EXPERIMENT DESIGN AND RESULTS

The experiment evaluates the pre-trained time-domain CNN models on software defined radio devices PLUTO for both LOS and NLOS channel scenarios in an indoor office with random people movement. Matlab software is installed and used in a personal computer (PC). Therefore, the CNN training and transfer learning are both within the PC but in the SDR device. The off-line CNN training is a one-time operation and the transfer learning is only activated when a device is re-located in a new environment.

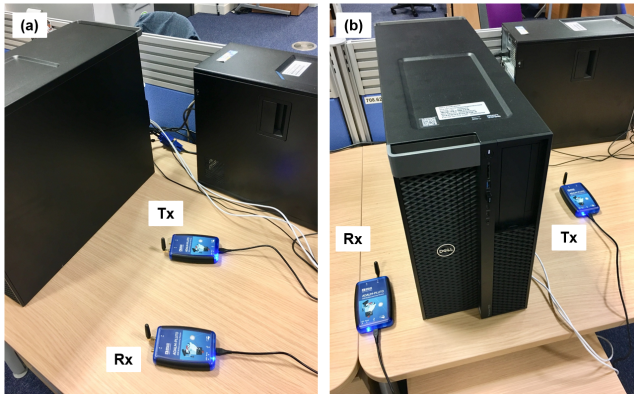


Fig. 5. PLUTO experiment. (a) Line-of-sight. (b) Non-line-of-sight.

A. Line-of-Sight Scenario

Two PLUTO devices are placed next to each other with 30 cm distance as demonstrated in Fig. 5(a). In addition, they are surrounded by two desktop hosts, which would introduce signal reflections. Therefore, there would be a main signal path that directly links the Tx antenna and Rx antenna with additional reflected signal paths. We generate 800 frames for each signal class at the Tx device for both Type-I and Type-II

signals. The Rx device receives the over-the-air signals at random intervals and it truncates time samples for classification.

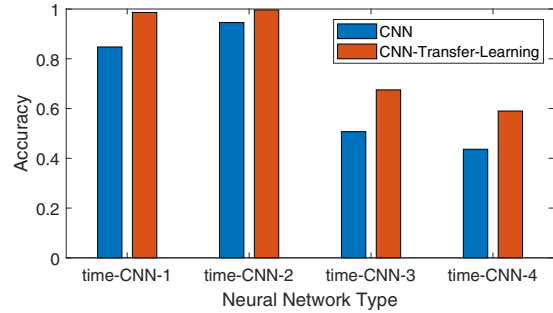


Fig. 6. Classification accuracy in the line-of-sight channel.

Results are shown in Fig. 6. First, similar to the results observed in Fig. 4, Type-I signal classification has higher accuracy than that in Type-II signals. Second, in Type-I signals, the CNN-2 model, trained with analytical channel/hardware impairments, shows a higher accuracy level than the pure signal trained CNN-1 model of no impairments. This agrees with the simulation results obtained from Fig. 4. For the Type-II signals, the pure signals trained CNN-3 outperforms the CNN-4 with impairments training. This result contradicts with the simulation results in Fig. 4. It is inferred that the mutual effect of signal similarity in Type-II signals and inaccurate channel/hardware impairments modelling has greater effect on classification accuracy than that for Type-I signals.

Transfer learning is applied for fine-tuning pre-trained neural networks. Training the entire neural network is time consuming and unrealistic for practical scenarios since a wireless channel would change frequently. Therefore, in this work only the last two layers of Fig. 2, concerned with extraction of channel features, are replaced; namely the full connection layer and SoftMax layer. In this case, the entire transfer learning would be faster. The receiver side PLUTO will collect 50 frames per signal class for re-training the last two layers. Practical results reveal that transfer learning greatly improves classification accuracy. For Type-I signals, the CNN-1 and CNN-2 models reach almost 100% accuracy. For Type-II signals, both CNN models are improved by up to 35% accuracy, but are still influenced strongly by the signal similarity. In a similar representation to that of [1], confusion matrices for CNN-1 are illustrated in Fig. 7, showing an evident accuracy improvement via the use of transfer learning.

B. Non-Line-of-Sight Scenario

Signal communications in NLOS are set up in Fig. 5 via placing obstacles between the transmitter and receiver. Results in Fig. 8 reveal that the classification accuracy levels for Type-I signals are still higher than those of Type-II signals even with obstacles blocking signal propagation. Applying transfer learning, the accuracy is further improved by up to 57%.

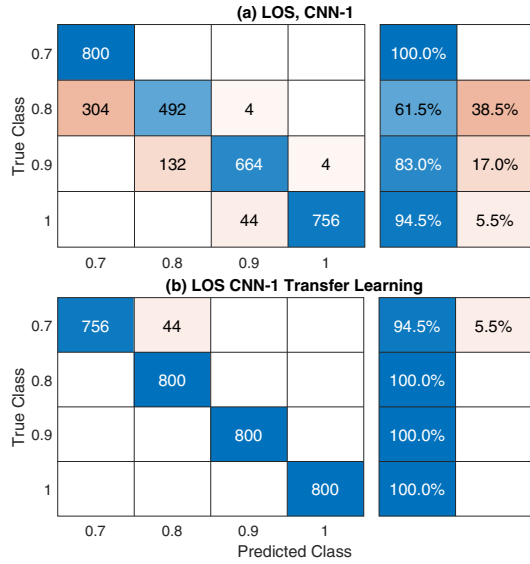


Fig. 7. Confusion matrix visualization. Type-I signal classification

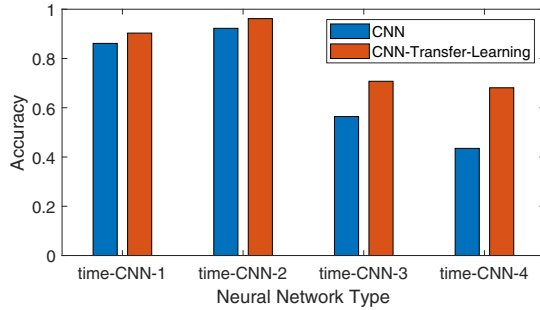


Fig. 8. Classification accuracy in the non-line-of-sight channel.

Table VI summarizes the numerical classification accuracy results for the different CNN models, communication scenarios and system testbeds.

Table VI: Classification accuracy for LOS and NLOS channels

Model	LOS		NLOS	
	Direct	Transfer learning	Direct	Transfer learning
CNN-1	84.75%	98.63%	86.13%	90.31%
CNN-2	94.56%	99.63%	92.25%	96.19%
CNN-3	50.71%	67.50%	56.43%	70.75%
CNN-4	43.64%	59.00%	43.50%	68.11%

V. CONCLUSION

This work deals with an intelligent signal classification task for non-orthogonal SEFDM signals in both simulation and over-the-air experiments. Unlike interference-free single-carrier and orthogonal multi-carrier OFDM signals, the sub-carriers within SEFDM are non-orthogonally packed leading to higher spectral efficiency at the cost of self-created interference. Therefore, classifying different SEFDM signals would be more challenging. Simulation results verify that the time-domain convolutional neural network (CNN) models

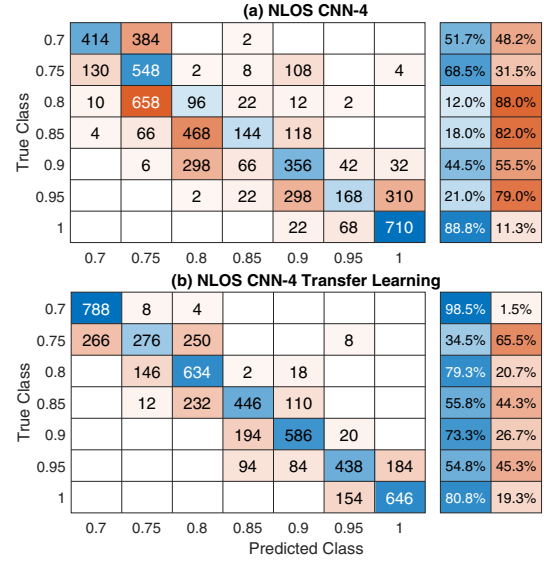


Fig. 9. Confusion matrix visualization. Type-II signal classification

outperform their frequency-domain models in classification accuracy. Experimental work with practical over-the-air testing is conducted using software defined radio devices in LOS and NLOS scenarios for various CNN models. A transfer learning strategy is applied to fine-tune the pre-trained models, showing classification accuracy ranged from 60% to nearly 100% with an improvement up to 57%. In summary, the feature-diversity dominant Type-I signals are suitable for non-cooperative communications while the feature-similarity dominant Type-II signals are potential for secure communications.

REFERENCES

- [1] T. J. O'Shea, T. Roy, and T. C. Clancy, "Over-the-air deep learning based radio signal classification," *IEEE Journal of Selected Topics in Signal Processing*, vol. 12, no. 1, pp. 168–179, Feb. 2018.
- [2] S. Zhou, Z. Yin, Z. Wu, Y. Chen, N. Zhao, and Z. Yang, "A robust modulation classification method using convolutional neural networks," *EURASIP Journal on Advances in Signal Processing*, pp. 1–15, 2019.
- [3] S. Hong, Y. Zhang, Y. Wang, H. Gu, G. Gui, and H. Sari, "Deep learning based signal modulation identification in OFDM systems," *IEEE Access*, 2019.
- [4] I. Darwazeh, H. Ghannam, and T. Xu, "The first 15 years of SEFDM: A brief survey," in *11th International Symposium on Communication Systems, Networks Digital Signal Processing (CSNDSP18)*, Jul. 2018, pp. 1–7.
- [5] J. Anderson, F. Rusek, and V. Öwall, "Faster-than-Nyquist signaling," *Proceedings of the IEEE*, vol. 101, no. 8, pp. 1817–1830, 2013.
- [6] T. Xu and I. Darwazeh, "Transmission experiment of bandwidth compressed carrier aggregation in a realistic fading channel," *IEEE Transactions on Vehicular Technology*, vol. 66, no. 5, pp. 4087–4097, May 2017.
- [7] S. J. Pan and Q. Yang, "A survey on transfer learning," *IEEE Transactions on Knowledge and Data Engineering*, vol. 22, no. 10, pp. 1345–1359, Oct. 2010.
- [8] T. J. O'Shea and N. West, "Radio machine learning dataset generation with GNU radio," *Proceedings of the 6th GNU Radio Conference*, 2016.
- [9] Analog-Devices, "ADALM-PLUTO SDR active learning module," <https://www.analog.com/media/en/news-marketing-collateral/product-highlight/ADALM-PLUTO-Product-Highlight.pdf>, technical document, Jul. 2019.
- [10] T. F. Collins, R. Getz, D. Pu, and A. M. Wyglinski, *Software-Defined Radio for Engineers*. Analog Devices, 2018.